

## Influence of B4C particle size on the mechanical behavior of A356 aluminium composites

Zeeshan Ali, V Muthuraman, P Rathnakumar, P Gurusamy, Madeva Nagaral

Online Publication Date: 30 Jan 2023

URL: <http://www.jresm.org/archive/resm2022.542ma1004tn.html>

DOI: <http://dx.doi.org/10.17515/resm2022.542ma1004tn>

Journal Abbreviation: *Res. Eng. Struct. Mater.*

### To cite this article

Ali Z, Muthuraman V, Rathnakumar P, Gurusamy P, Nagaral M. Influence of B4C particle size on the mechanical behavior of A356 aluminium composites. *Res. Eng. Struct. Mater.*, 2023; 9(2): 527-540.

### Disclaimer

All the opinions and statements expressed in the papers are on the responsibility of author(s) and are not to be regarded as those of the journal of Research on Engineering Structures and Materials (RESM) organization or related parties. The publishers make no warranty, explicit or implied, or make any representation with respect to the contents of any article will be complete or accurate or up to date. The accuracy of any instructions, equations, or other information should be independently verified. The publisher and related parties shall not be liable for any loss, actions, claims, proceedings, demand or costs or damages whatsoever or howsoever caused arising directly or indirectly in connection with use of the information given in the journal or related means.



Published articles are freely available to users under the terms of Creative Commons Attribution - NonCommercial 4.0 International Public License, as currently displayed at [here](https://creativecommons.org/licenses/by-nc/4.0/) (the "CC BY - NC").



Technical Note

## Influence of B<sub>4</sub>C particle size on the mechanical behavior of A356 aluminium composites

Zeeshan Ali<sup>1,a</sup>, V Muthuraman<sup>2,b</sup>, P Rathnakumar<sup>1,c</sup>, P Gurusamy<sup>3,d</sup>, Madeva Nagaral<sup>4,e</sup>

<sup>1</sup>Department of Mechanical Engineering, Navodaya Institute of Technology, Raichur, Karnataka, India

<sup>2</sup>Vels Institute of Science, Technology and Advanced Studies, Chennai, India

<sup>3</sup>Department of Mechanical Engineering, Chennai Institute of Technology, Chennai, India

<sup>4</sup>Aircraft Research and Design Centre, HAL, Bengaluru, Karnataka, India

### Article Info

#### Article history:

Received 04 Dec 2022

Revised 12 Jan 2023

Accepted 27 Jan 2023

#### Keywords:

A356 Alloy;

B<sub>4</sub>C;

SEM;

EDS;

Tensile Strength;

Compressive Strength;

Impact Toughness

### Abstract

The influence of adding B<sub>4</sub>C particulates with a 40 and 90 μm sizes on the compressive strength, tensile strength and impact toughness of the A356 alloy is being studied. In the Al alloy matrix, 40 and 90 μm -sized micro B<sub>4</sub>C particulates are employed as reinforcements. In the A356 alloy, composites are created utilizing the liquid melt process in increments of 3 and 6 weight percent. Using an energy dispersive spectroscopy (EDS) and a scanning electron microscope (SEM), samples are examined for microstructural characterization. According to ASTM standards, mechanical characteristics including tensile, hardness, compression, and toughness are assessed. The consistent distribution of B<sub>4</sub>C particles in the A356 alloy is seen in SEM micrographs, and this is supported by EDS analysis. Additionally, the inclusion of B<sub>4</sub>C reinforcement improves the compression and impact strength of the base matrix A356 alloy, which is especially noticeable in the case of reinforced composites that are 6 wt. % of 40 μm B<sub>4</sub>C in size.

© 2023 MIM Research Group. All rights reserved.

## 1. Introduction

Due to its beneficial qualities, such as light weight, corrosion resistance, high stiffness, and cost efficiency when compared to currently utilized metals, aluminum is extensively employed in aerospace, automotive, and structural applications. Aluminum has a density that is around one-third that of iron and copper, and its corrosion resistance negates the need for protective coatings. Recent growth in research suggests that there is still more room for advancement in the use of aluminum. Utilizing aluminum with increased characteristics will satisfy both economic and environmental needs [1].

Aluminum metal matrix composites (AMMC) may be treated in a number of ways, including liquid metallurgy, solid metallurgy, in situ procedures, etc. However, liquid metallurgy is preferred owing to its cheap cost, ease of processing, and superior characteristics. The primary issue with processing AMMC is the wettability of the ceramic particles, which may be solved by coating the reinforcement, which is one of the methods to improve wettability [2]. Ti coating has shown superior results for improving the wettability of B<sub>4</sub>C. By creating a thin coating of Ti around the B<sub>4</sub>C particles, the K<sub>2</sub>TiF<sub>6</sub> halide salt, which is evenly mixed with B<sub>4</sub>C during casting, has improved the bonding between Al and B<sub>4</sub>C and the mechanical characteristics of the material. Aluminum is combined with B<sub>4</sub>C and graphite using a mechanical stirrer. The homogenous dispersion of particles in the metal matrix is facilitated by the use of a mechanical stirrer and

\*Corresponding author: [madev.nagaral@gmail.com](mailto:madev.nagaral@gmail.com)

<sup>a</sup> [orcid.org/0000-0002-7439-6656](https://orcid.org/0000-0002-7439-6656); <sup>b</sup> [orcid.org/0000-0001-9891-0165](https://orcid.org/0000-0001-9891-0165); <sup>c</sup> [orcid.org/0000-0003-2768-4601](https://orcid.org/0000-0003-2768-4601);

<sup>d</sup> [orcid.org/0000-0003-1641-9415](https://orcid.org/0000-0003-1641-9415); <sup>e</sup> [orcid.org/0000-0002-8248-7603](https://orcid.org/0000-0002-8248-7603)

DOI: <http://dx.doi.org/10.17515/resm2022.542ma1004tn>

Res. Eng. Struct. Mat. Vol. 9 Iss. 2 (2023) 527-540

vigorous stirring. In liquid metallurgy, reinforcing particles are added in two steps, assisting with homogenous distribution and preventing particulate aggregation [3].

In general, aluminum-based MMCs provide a significant improvement in elasticity modulus, strength, and wear resistance compared to unreinforced alloys. The reinforcing particle size, shape, and volume fraction, the matrix material, and the response at the interface all have an impact on the properties of composites. Hard ceramic particles such as SiO<sub>2</sub>, SiC, Al<sub>2</sub>O<sub>3</sub>, TiB<sub>2</sub>, B<sub>4</sub>C, etc. may be added to the Al matrix to reinforce it and increase its characteristics [4]. Al<sub>2</sub>O<sub>3</sub> and SiC ceramic particles are the most often utilized materials for aluminum reinforcement. Due to its great hardness it is the third hardest substance after diamond and boron nitride boron carbide (B<sub>4</sub>C) might be used as a replacement to silica and aluminum oxide [5]. High strength, low density, exceptionally high hardness, strong wear resistance, and good chemical stability are some of B<sub>4</sub>C's appealing qualities. As a result, B<sub>4</sub>C particle reinforcement of aluminum results in increased specific strength, elastic modulus, wear resistance, and thermal stability [6].

According to the literature review, SiC and Al<sub>2</sub>O<sub>3</sub> particle reinforcements are the focus of the majority of investigations on aluminum-based MMCs. TiC particulate reinforcement of aluminum matrix is, however, comparatively underutilized. Despite the fact that powder metallurgy gives MMCs higher mechanical characteristics, liquid state processing offers certain significant benefits. Better matrix-particle bonding, simpler matrix structure management, cheap processing costs, closer net form, and a broad range of material options are a few of them. There are two techniques for manufacturing MMCs in a liquid state, and they are both dependent on the temperature at which the particles are added to the melt. The vortex is utilized to introduce reinforcement particles in both processes. Micro-particles are particularly cost-effective due to their cheap cost and simplicity of dispersion during manufacturing.

Stir casting is considered as the most effective and cost-effective technique out of all of them. However, this technique has always resulted in a large number of structural flaws in composite materials. Some significant structural flaws of stir cast composites include poor wettability, uneven distribution of reinforcement particles, segregation and agglomeration of reinforcement [7]. The compressive and impact characteristics of the A356 reinforced with micron B<sub>4</sub>C particles MMC's manufactured by stir casting technique, however, are little understood. Aluminum-boron carbide composites are crucial, particularly in the aerospace industry, where there is a growing need for lightweight materials. The development of A356 micron B<sub>4</sub>C composites with different particle sizes and weight percentages of B<sub>4</sub>C particulates is suggested in light of the aforementioned findings.

In this work, the mechanical characteristics of A356 alloy-based composites containing 40 and 90 μm sized B<sub>4</sub>C particles were examined utilizing the liquid metallurgical process at different weight percentages (3 and 6 wt. % B<sub>4</sub>C). Based on the literature, smaller particles create agglomeration in the prepared composites, whereas larger particle addition creates de-bonding particles from the matrix. Hence, an attempt was made to develop an A356 alloy with varying boron carbide particle-reinforced composites and investigate the effect of the optimum reinforcing particle size on the mechanical properties of the composites.

## 2. Experimental Details

By using liquid metallurgy, metal matrix composites with 3 and 6 wt. % of B<sub>4</sub>C particles and size of 40 and 90 μm are created. A356 alloy is employed as the matrix material and B<sub>4</sub>C particles with an average size of 40 μm are used as reinforcements in the fabrication

of MMCs. Table 1 is showing chemical composition of A356 alloy and Table 2 is representing chemistry of  $B_4C$  particles.

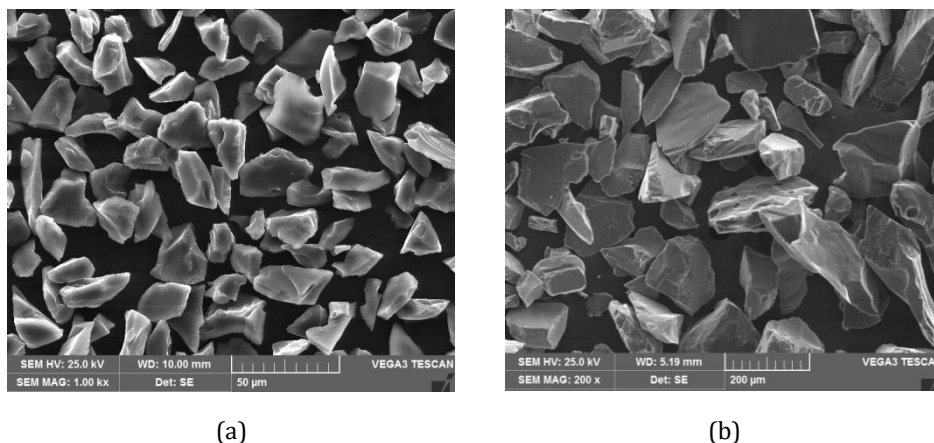


Fig.1 SEM images of (a) 40  $\mu m$   $B_4C$  (b) 90  $\mu m$   $B_4C$  particles

Table 1. Chemical Composition of A356 Alloy

Element	Symbol	Wt %
Silicon	Si	6.98
Magnesium	Mg	0.35
Iron	Fe	0.10
Titanium	Ti	0.15
Copper	Cu	0.01
Nickel	Ni	0.013
Zinc	Zn	<0.015
Tin	Sn	<0.005
Manganese	Mn	<0.005
Aluminum	Al	Balance

Table 2. Chemical composition of  $B_4C$

Total Boron	Total Carbon	Total Iron	Total Boron + Carbon
77.5%	21.5%	0.2%	99.8%

## 2.1. Preparation of Composites

A356 alloy with 40 and 90 micron sized  $B_4C$  particles reinforced composites were created using the liquid metallurgical approach. An A356 alloy ingots were charged into the furnace by taking calculated quantity to melt. A356 alloy has a 660°C melting temperature. The maximum melting temperature of 750°C was used to melt the A356 alloy. A chromel-alumel thermocouple was used to measure the temperature. Hexachloroethane ( $C_2Cl_6$ ) in solid form was then used to degas the liquid metal or remove the unwanted gases from the molten metal. The molten metal was stirred to form a vortex using a zirconium-coated stainless-steel impeller. The impeller was immersed 60 % below the height of the molten metal from the melt's surface and the stirrer rotates at a speed of 300 rpm. The pre-heated  $B_4C$  particles were added to the vortex. The A356 alloy with 3 weight percentage of  $B_4C$  composites were then placed into a permanent cast

iron mould with dimensions of 120 mm in length and 15 mm in diameter [8]. Similarly, A356 alloy with 6 wt. % of boron carbide particles reinforced composites were synthesized in the similar way. Further, based on the microstructural analysis, the tensile strength, hardness, compressive strength and impact toughness of the A356 alloy of 40 and 90  $\mu\text{m}$  sized  $\text{B}_4\text{C}$  reinforced composites were evaluated and compared with the as-cast A356 alloy. Figure 2 shows cast aluminum specimen.



Fig. 2 Cast aluminum specimen

## 2.2. Testing of Composites

The microstructural specimens were polished using 220 to 1000 grit emery sheets before being subjected to diamond paste polishing and microstructural examination by SEM and EDS [9]. The specimens were etched with Keller's reagent. According to ASTM E10 standard, the hardness test was performed using Brinell hardness testing equipment. ASTM E8 and E9 standards were used to conduct the tensile and compression tests. According to ASTM E23 standard, the Charpy impact test was performed using an impact test machine.

## 3. Results and Discussion

### 3.1. Microstructural Study

The microstructure of the cast A356 aluminum alloy is seen in Fig. 3(a). A356 composites with 40 and 90  $\mu\text{m}$  sized particles of 3% and 6% wt.%  $\text{B}_4\text{C}$  content are shown in Fig. 3(b-e). As shown in figures, the SEM micrographs show a very equal distribution of  $\text{B}_4\text{C}$  particles throughout the matrices (Fig. 3b-e). The porosity of the MMC is decreased by uniformly dispersed particles, which also improve overall strength and other qualities. From the micrographs it is revealed that the boron carbide particles distributed uniformly in the matrix material. The bonding between the A356 alloy and boron carbide particles is strong and helps in enhancing the properties.

Energy dispersive spectrographs (EDS) of the cast A356 aluminum alloy is seen in Fig. 4 (a) A356-3 wt.% of 40 and 90  $\mu\text{m}$  sized  $\text{B}_4\text{C}$  particulates reinforced composites, and A356-6 wt. % of 40 and 90  $\mu\text{m}$  sized  $\text{B}_4\text{C}$  particulates reinforced composites are shown in Fig. 4 (b-e). The B (Boron) and C (Carbon) components in the composites help to identify the presence of  $\text{B}_4\text{C}$  particles.

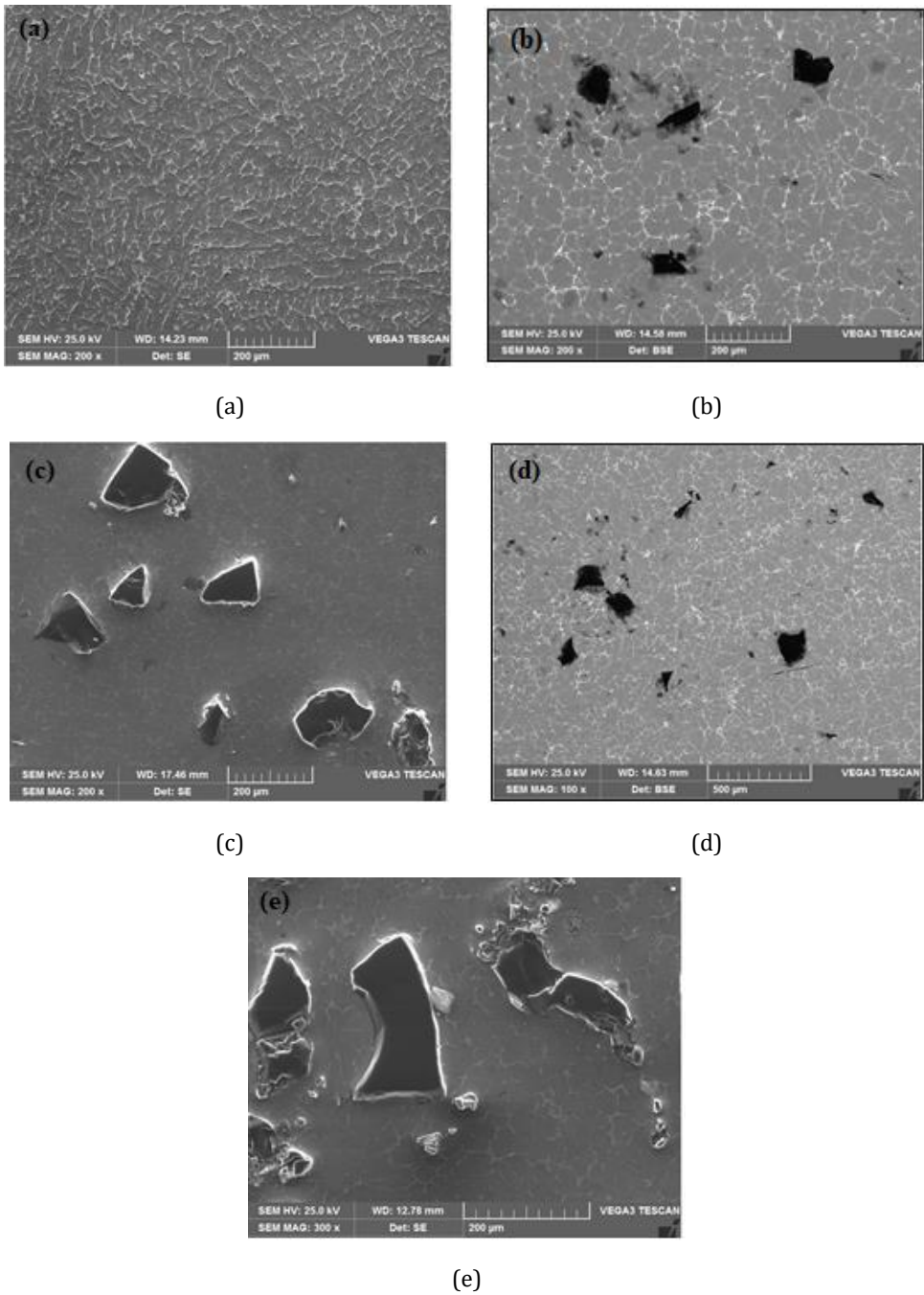
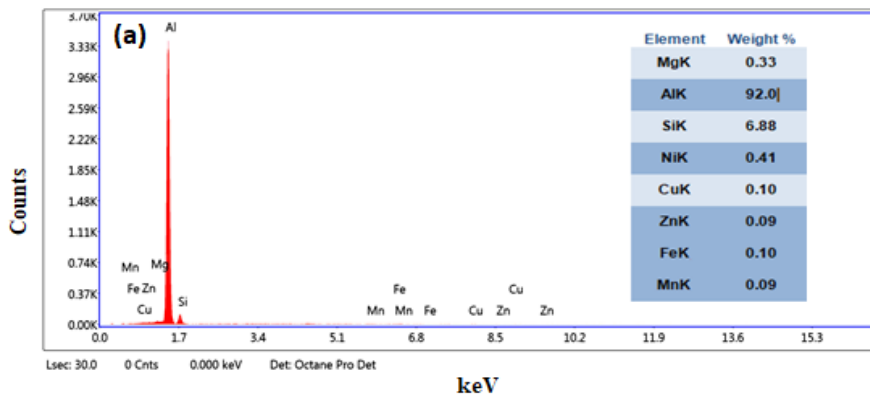
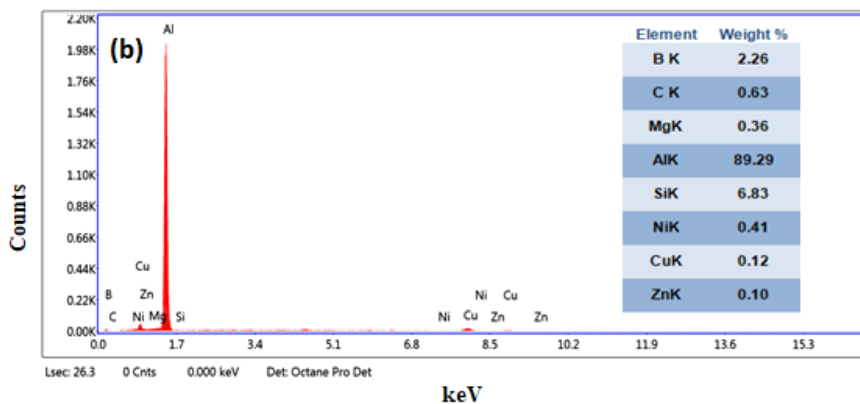


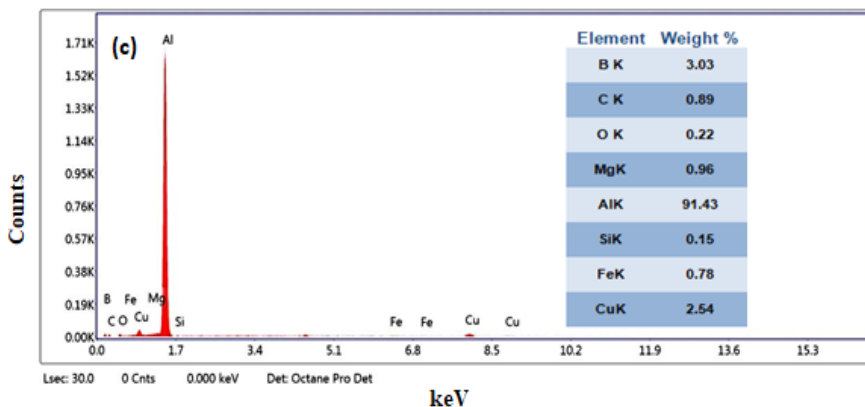
Fig. 3 SEM image of a) A356 alloy b) 3 wt.% 40µm B<sub>4</sub>C c) 3 wt.% 90µm B<sub>4</sub>C d) 6 wt.% 40µm B<sub>4</sub>C e) 6 wt.% 90µm B<sub>4</sub>C



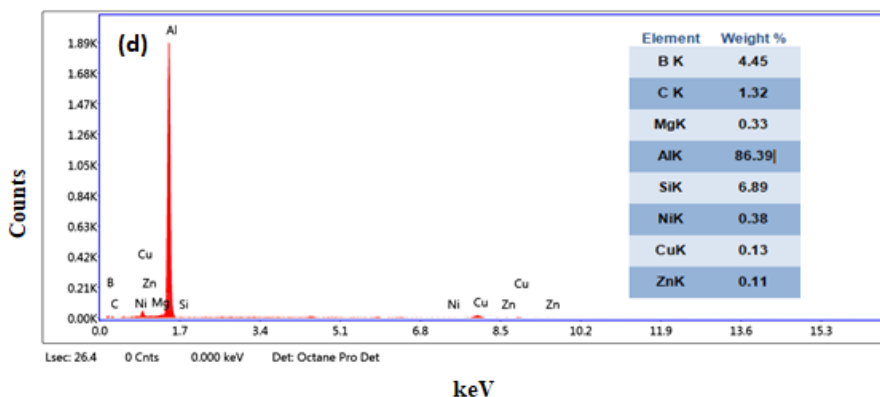
(a)



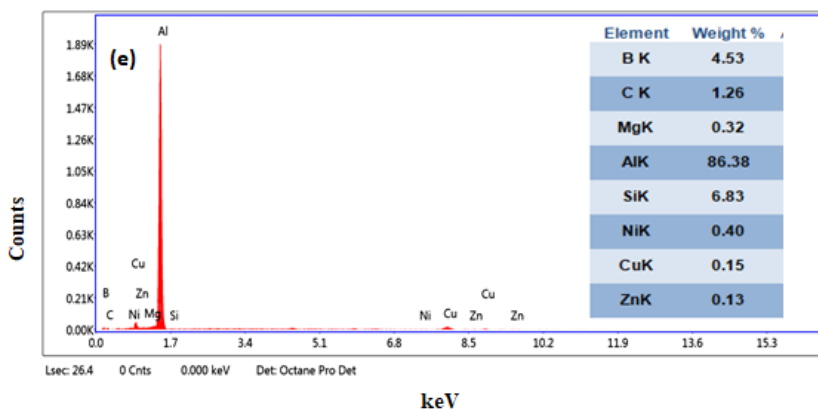
(b)



(c)



(d)



(e)

Fig. 4 SEM image of a) A356 alloy b) 3 wt.% 40µm B<sub>4</sub>C c) 3 wt.% 90µm B<sub>4</sub>C d) 6 wt.% 40µm B<sub>4</sub>C e) 6 wt.% 90µm B<sub>4</sub>C

### 3.2. Tensile Properties

To analyze tensile parameters such as ultimate tensile strength and yield strength, the tensile behavior of all the composite sample preparations is determined. The computerized universal testing apparatus received the specimens by hydraulic loading. The weights that caused the specimen to break and reach the yield point were noted. Fig. 5, 6 and Table 3 depicts how adding B<sub>4</sub>C particles of 40 and 90 µm in size affected the samples' ultimate tensile strength and yield strength. In a nutshell, both direct and indirect strengthening plays a significant role in the strengthening [10]. With the addition of 6 wt. % 40 and 90 µm size B<sub>4</sub>C, the ultimate tensile strength and yield strength both exhibit an improvement. This improvement is mostly attributable to an increase in dislocation density and their accumulation behind the uniformly dispersed B<sub>4</sub>C. The changes in the matrix microstructure brought on by the presence of reinforcement particles lead to indirect strengthening. The mismatch in the coefficient of thermal expansion between B<sub>4</sub>C and A356 alloy causes an increase in dislocation density in the A356- B<sub>4</sub>C composites, which leads to indirect strengthening [11]. As the weight

percentage of B<sub>4</sub>C rises, so does the density of these thermally generated dislocations, increasing the indirect strengthening contribution as well. On the other hand, work hardening behavior seems to be the cause of this progressive improvement.

Table 3. Tensile properties of A356 alloy and its B<sub>4</sub>C composites with standard deviation

Material Composition	B <sub>4</sub> C Particle Size (micron)	Ultimate Tensile Strength (MPa)	Yield Strength (MPa)
A356 Alloy	--	162.5 ± 0.95	126.4 ± 1.11
A356 - 3 wt. % B <sub>4</sub> C	40	183.2 ± 0.75	151.4 ± 1.02
A356 - 6 wt. % B <sub>4</sub> C		206.4 ± 1.10	182.0 ± 0.72
A356 - 3 wt. % B <sub>4</sub> C	90	179.2 ± 1.01	148.2 ± 1.15
A356 - 6 wt. % B <sub>4</sub> C		198.4 ± 1.07	168.7 ± 0.76

± - SD (Standard Deviation)

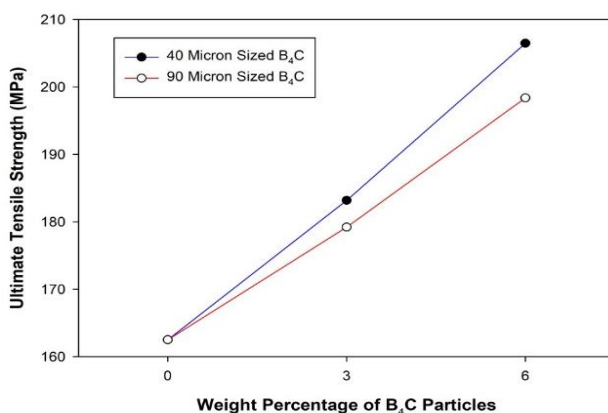


Fig. 5 Ultimate tensile strength of A356 with B<sub>4</sub>C composites

In composite materials, the presence of a larger weight percentage of B<sub>4</sub>C boosted the strengthening effect and load absorption. When compared to the unreinforced A356 alloy, the aluminum alloy containing reinforcement particles such boron carbide reinforcement supplied the highest tensile strength, according to earlier study findings [12]. Particle reinforcement increased strength and provided greater resilience to tensile stresses. The highest tensile strength of composites is provided through load transmission from the matrix to the reinforcing particles.

If an applied stress at which considerable internal damage (particle fracture and/or interfacial failure) occurs is taken into account, the impact of reinforcement as a function of matrix yield stress and tensile strength may be somewhat rationalized. The distribution of residual tension and the size of the particles are two important variables that will affect this stress. The impact of particle size is significant since the average fracture stress of the B<sub>4</sub>C particles decreases as particle size rises. Therefore, in composites reinforced with big particles, particle breakage will occur at lower applied stress levels and therefore, will be reduced. Additionally, the overall interfacial area will shrink as particle size rises. Particle size is unlikely to have a significant impact on the interfacial strength. Therefore, when the particle size rises, the percentage of particle damage caused by particle breakage is anticipated to rise.

The uniformity of the particle dispersion may have an impact on the tensile characteristics of these materials. These have been shown to be quite homogenous in the current situation (Fig. 3b-e), and it is thought that they will not significantly affect the trends of the current work. The presence of any clusters, however, may impair strength and ductility by causing localized damage. Such clusters might be seen in this context as areas of potential harm that exist before loading. It should be emphasized that composites reinforced with small particulates, which seem to have more strength and ductility than materials containing coarse particles, are often more prone to have any such clustering. It is obvious that any such zones of clustering must be minimized if optimal performance is sought, particularly for the tiny particle reinforced composites.

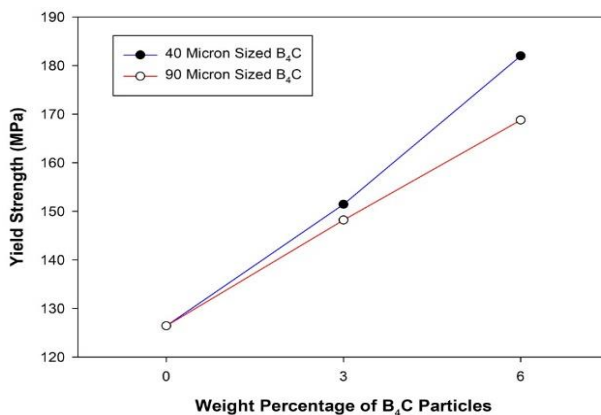


Fig. 6 Yield strength of A356 with B<sub>4</sub>C composites

### 3.3. Hardness Measurements

Brinell hardness tester was used to measure the composites' hardness. Test specimens were carved out of each composite composition and polished before testing in order to achieve a flat and smooth surface finish. Brinell hardness is assessed by pressing a hard steel or carbide sphere with a certain diameter into a material's surface under a predetermined force for a predetermined amount of time, then measuring the diameter of the indentation that remains after the test. By dividing the applied force, in kilograms, by the actual surface area of the indentation, in square millimeters, one may get the Brinell hardness number. For aluminum castings, a 500 kilograms load is applied for 30 seconds. Each sample underwent several hardness tests, with the average result used to calculate the specimen's hardness.

Fig. 7 and Table 4 compares the hardness of A356 alloy with composites supplemented with 40 and 90  $\mu\text{m}$  sized B<sub>4</sub>C particulates at 3 and 6 weight percentages. The graph clearly shows that the hardness of the A356 alloy in both 40 and 90  $\mu\text{m}$  of 3 and 6 wt. percent sized composites rises as the weight percentage of reinforcing particles increases [13, 14]. The basic matrix A356 alloy has a hardness of 60.3 BHN. The hardness of A356 alloy is 65.4 BHN with 3 wt. percent of 40  $\mu\text{m}$  B<sub>4</sub>C particle reinforced composites, and it is 76.3 BHN with 6 wt. percent of 40  $\mu\text{m}$  B<sub>4</sub>C particle reinforced composites. Similarly, in the case of 3 and 6 weight percentages of 90  $\mu\text{m}$  sized B<sub>4</sub>C particulates reinforced A356 alloy composites it is 64.1 and 73 BHN respectively.

Table 4. Hardness of A356 alloy and its B<sub>4</sub>C composites with standard deviation

Material Composition	B <sub>4</sub> C Particle Size (micron)	Hardness (BHN)
A356 Alloy	--	60.33 ± 1.22
A356 – 3 wt. % B <sub>4</sub> C	40	65.43 ± 0.80
A356 – 6 wt. % B <sub>4</sub> C		76.30 ± 1.05
A356 – 3 wt. % B <sub>4</sub> C	90	64.13 ± 1.00
A356 – 6 wt. % B <sub>4</sub> C		73.03 ± 0.77

± - SD (Standard Deviation)

The data show that the hardness of B<sub>4</sub>C composites with a 40 μm size 6 wt. % is greater than that of B<sub>4</sub>C composites with 3 wt. %. The improvement in hardness is more pronounced in composites supplemented with smaller particle and larger in quantity. This enhancement is caused by the particles' excellent wettability in the matrix of the A356 alloy and is also evident from microstructural tests. The bonding between the reinforcement and the matrix alloy increases as particle size decreases [15, 16].

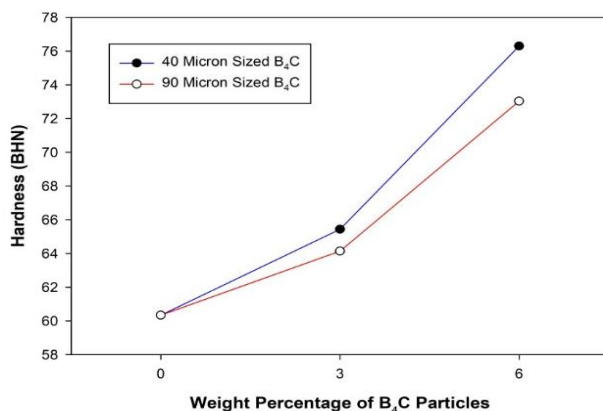


Fig. 7 Hardness of A356 with B<sub>4</sub>C composites

### 3.4. Compression Strength

The Universal Testing Machine does compression testing (UTM). On the UTM's base plate is affixed the cylindrical test specimen. The specimen being utilized has a diameter that is equal to its height. The specimen is progressively loaded until it has been crushed by 50% (height). When applying higher weights, displacement also rises up to a certain point before abruptly falling till it reaches a height beyond which it can no longer be squeezed.

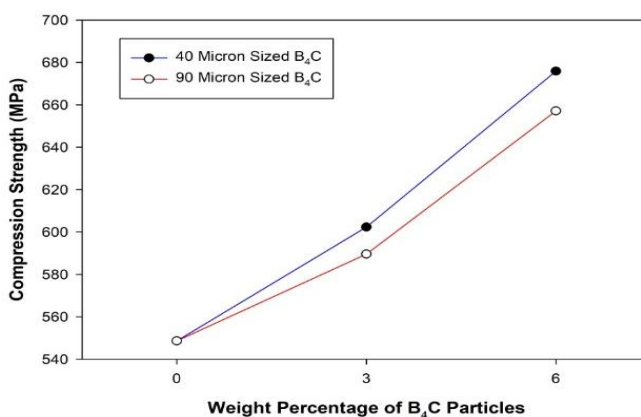
Fig. 8 and Table 5 compares the compressive strength of composites reinforced with 3 and 6 weight percent of 40 and 90 μm B<sub>4</sub>C particles with that of A356 alloy. When B<sub>4</sub>C particles with sizes of 40 and 90 μm are added, the compressive strength of the A356 alloy rises. Furthermore, as compared to composites reinforced with 40 μm sized B<sub>4</sub>C particulates exhibit better compressive strength. The basic matrix of the A356 alloy has a compressive strength of 548.6 MPa.

Table 5. Compression strength of A356 alloy and its B<sub>4</sub>C composites with standard deviation

Material Composition	B <sub>4</sub> C Particle Size (micron)	Compression Strength (MPa)
A356 Alloy	--	548.60 ± 2.36
A356 – 3 wt. % B <sub>4</sub> C	40	602.33 ± 3.51
A356 – 6 wt. % B <sub>4</sub> C	40	675.87 ± 3.25
A356 – 3 wt. % B <sub>4</sub> C	90	589.57 ± 3.10
A356 – 6 wt. % B <sub>4</sub> C	90	657.13 ± 4.17

± - SD (Standard Deviation)

The compressive strength of A356 alloy is 602.3 MPa with 3 wt. percent of 40 μm B<sub>4</sub>C particle reinforced composites, and it is 675.9 MPa with 6 wt. percent of 40 μm B<sub>4</sub>C particle reinforced composites. Similarly, in the case of 3 and 6 weight percentages of 90 μm sized B<sub>4</sub>C particulates reinforced A356 alloy composites it is 589.6 and 657.1 respectively. This improvement is the result of the matrix's hard B<sub>4</sub>C particles, which have a higher compressive strength [17, 18]. Additionally, the higher resistance of crushing 40 μm 6 wt. % B<sub>4</sub>C particles is the reason for the increased strength in 40 μm sized particle reinforced composites as compared to 3 wt. % reinforced composites.

Fig. 8 Compression strength of A356 with B<sub>4</sub>C composites

### 3.5. Impact Strength

Fig. 9 and Table 6 compares the impact toughness of A356 alloy with 40 and 90 μm sized B<sub>4</sub>C reinforced composites. In reinforced composites with 40 and 90 μm sized particle sizes, the impact toughness of the A356 alloy is enhanced by 3 and 6 weight percent. A356 alloy with 6 weight percent Boron carbide in 40 μm composites demonstrate greater impact toughness than composites with 3 weight percent B<sub>4</sub>C particles. The greater resistance of smaller particles to debonding during impact loading accounts for the majority of the improvement in impact toughness in 40 μm B<sub>4</sub>C composites.

There is no void formation or debonding at the interface of the matrix and the particle reinforcements, indicating improved interfacial bonding between the matrix and the reinforcements [19, 20]. The uniformity produced by the homogeneous dispersion of B<sub>4</sub>C particles in the matrix improves the matrix-reinforcement bonding as well as the impact

strength of composites. Under the impact loading, the homogeneous particles could clearly be distinguished. The SEM analyses in figure 3 lend credence to this hypothesis.

As a result, particle cracking dominates the failure mechanism. This outcome is consistent with the literature, which states that particle breakage occurs when the contact is stronger than the individual particles. Therefore, it seems that the failure results from an accumulation of internal damage brought on by particle breakage and matrix material deformation [21, 22].

Table 6. Impact strength of A356 alloy and its B<sub>4</sub>C composites with standard deviation

Material Composition	B <sub>4</sub> C Particle Size (micron)	Impact Strength (J)
A356 Alloy	--	1.10 ± 0.1
A356 – 3 wt. % B <sub>4</sub> C	40	1.45 ± 0.05
A356 – 6 wt. % B <sub>4</sub> C		1.90 ± 0.03
A356 – 3 wt. % B <sub>4</sub> C	90	1.35 ± 0.04
A356 – 6 wt. % B <sub>4</sub> C		1.88 ± 0.02

± - SD (Standard Deviation)

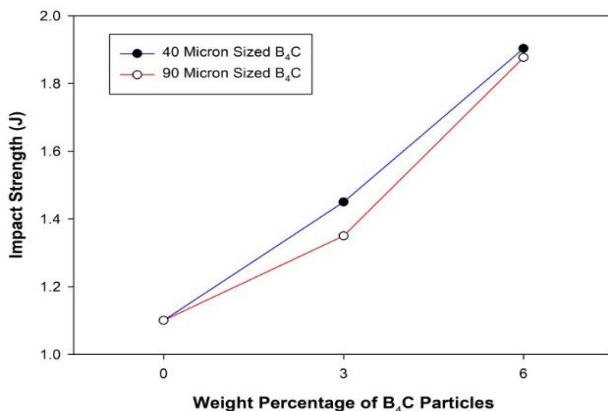


Fig. 9 Impact strength of A356 with B<sub>4</sub>C composites

#### 4. Conclusions

The following general findings are drawn from this study on the synthesis and characterization of composites reinforced with B<sub>4</sub>C particles of various sizes made of the A356 alloy:

- Stir casting is an effective method for producing reinforced composites made of A356 alloy that include 3 and 6 weight percent of B<sub>4</sub>C particulates that are 40 and 90 μm in size.
- Energy dispersive analysis (EDS) confirms the existence of B<sub>4</sub>C particles in the form of C elements in composites made of A356 and B<sub>4</sub>C that are 40 and 90 μm in size.
- SEM micrographs show a very equal distribution of B<sub>4</sub>C particles throughout the matrix.
- The inclusion of 40 and 90 μm sized B<sub>4</sub>C particles enhances the tensile properties of A356 composites with 3 and 6 wt.%B<sub>4</sub>C. Additionally, as cast A356

alloy and composites reinforced with 6 wt.% percent 40  $\mu\text{m}$  sized  $\text{B}_4\text{C}$  particles exhibit better tensile properties than composites reinforced with 3 wt.%  $\text{B}_4\text{C}$ . The inclusion of 40 and 90  $\mu\text{m}$  sized  $\text{B}_4\text{C}$  particles enhances the hardness of A356 composites with 3 and 6 wt.%  $\text{B}_4\text{C}$ . Additionally, as cast A356 alloy and composites reinforced with 6 wt.% percent 40  $\mu\text{m}$  sized  $\text{B}_4\text{C}$  particles exhibit better hardness than composites reinforced with 3 wt.%  $\text{B}_4\text{C}$ . The addition of  $\text{B}_4\text{C}$  particles results in an increase in the compressive strength of the A356 matrix. Furthermore, compared to 3 wt. %  $\text{B}_4\text{C}$  composites, the A356 alloy with 6 wt. % 40  $\mu\text{m}$  sized  $\text{B}_4\text{C}$  particle reinforced composites show greater compressive strength.

- The inclusion of  $\text{B}_4\text{C}$  particles increases the impact toughness of the A356 matrix. Furthermore, compared to 3 wt. % 40  $\mu\text{m}$  sized  $\text{B}_4\text{C}$  composites, the A356 alloy supplemented with 6 wt.% percent 40  $\mu\text{m}$  sized  $\text{B}_4\text{C}$  particle demonstrates greater impact toughness.

## References

- [1] Bharath V, Auradi V, Nagal M. Fractographic characterization of  $\text{Al}_2\text{O}_3$  particulates reinforced Al2014 alloy composites subjected to tensile loading. *Frattura ed Integrità Strutturale*, 2021; 15(57): 14-23. <https://doi.org/10.3221/IGF-ESIS.57.02>
- [2] Harti J, Prasad TB, Nagal M, Rao KN. Hardness and tensile behavior of Al2219-TiC metal matrix composites. *Journal of Mechanical Engineering and Automation*, 2016; 6(5A): 8-12.
- [3] Ali Z, Muthuraman V, Rathnakumar P, Gurusamy P, Nagal M. Investigation on the tribological properties of copper alloy reinforced with Gr/ZrO<sub>2</sub> particulates by stir casting route. *Materials Today: Proceedings*, 2020; 33: 3449-3453. <https://doi.org/10.1016/j.matpr.2020.05.351>
- [4] Balaraj V, Nagaraj K, Nagal M, Auradi V. Microstructural evolution and mechanical characterization of micro  $\text{Al}_2\text{O}_3$  particles reinforced Al6061 alloy metal composites. *Materials Today: Proceedings*, 2021; 47: 5959-5965. <https://doi.org/10.1016/j.matpr.2021.04.500>
- [5] Ali Z, Muthuraman V, Rathnakumar P, Gurusamy P, Nagal M. Studies on mechanical properties of 3 wt.% of 40 and 90  $\mu\text{m}$  size  $\text{B}_4\text{C}$  particulates reinforced A356 alloy composites. *Materials Today: Proceedings*, 2022; 52: 494-499. <https://doi.org/10.1016/j.matpr.2021.09.260>
- [6] Gurusamy P, Muthuraman V, Raj SHK, Kumar JL. Performance and experimental analysis of Al- $\text{Al}_2\text{O}_3$  metal matrix composites. *International Journal of Vehicle Structures & Systems*, 2022; 14(2): 257-259. <https://doi.org/10.4273/ijvss.14.2.20>
- [7] Shetty RP, Mahesh TS, Ali Z, Veerasha G, Nagal M. Studies on mechanical behavior and tensile fractography of boron carbide particles reinforced Al8081 alloy advanced metal composites. *Materials Today: Proceedings*, 2022; 52: 2115-2120. <https://doi.org/10.1016/j.matpr.2021.12.397>
- [8] Nagal M, Auradi V, Kori SA, Reddappa HN, Jayachandran, Shivaprasad V. Studies on 3 and 9 wt. % of  $\text{B}_4\text{C}$  particulates reinforced Al7025 alloy composites. In *AIP Conference Proceedings*, 2017; 1859, 1: 020019. <https://doi.org/10.1063/1.4990172>
- [9] Prasad GP, Chittappa HC, Nagal M, Auradi V. Influence of  $\text{B}_4\text{C}$  reinforcement particles with varying sizes on the tensile failure and fractography of LM29 alloy composites. *Journal of Failure Analysis and Prevention*, 2020; 20(6): 2078-2088. <https://doi.org/10.1007/s11668-020-01021-6>
- [10] Nithin K, Kumar HS, Hemanth RT, Nagal M, Auradi V, Veerasha RK. Microstructural characterization, mechanical and taguchi wear behavior of micro-titanium carbide particle-reinforced Al2014 alloy composites synthesized by advanced two-stage

- casting method. Journal of Bio and Tribo-Corrosion, 2022;8(109):1-16. <https://doi.org/10.1007/s40735-022-00709-6>
- [11] Krishna Prasad S, Samuel Dayanand, Rajesh , Madeva Nagaral, Auradi V, Rabin Selvaraj. Preparation and Mechanical Characterization of TiC Particles Reinforced Al7075 Alloy Composites, Advances in Materials Science and Engineering, 2022, Article ID 7105189, <https://doi.org/10.1155/2022/7105189>
- [12] Kumar HSV, Kempaiah UN, Nagaral M. Impact, tensile and fatigue failure analysis of boron carbide particles reinforced Al-Mg-Si (Al6061) alloy composites. Journal of Failure Analysis and Prevention, 2021; 21: 2177-2189. <https://doi.org/10.1007/s11668-021-01265-w>
- [13] Nagaral M, Deshapande RG, Auradi V, Satish BP, Samuel D, Anilkumar MR. Mechanical and wear characterization of ceramic boron carbide-reinforced Al2024 alloy metal composites. Journal of Bio-and Tribo-Corrosion, 2021; 7(1):1-12. <https://doi.org/10.1007/s40735-020-00454-8>
- [14] Nagaral M, Auradi V, Kori SA, Vijaykumar H. Investigations on mechanical and wear behavior of nano Al2O3 particulates reinforced AA7475 alloy composites. Journal of Mechanical Engineering and Sciences, 2019; 13(1):4623-4635. <https://doi.org/10.15282/jmes.13.1.2019.19.0389>
- [15] Pankaj RJ, Nagaral M, Shivakumar R, Jayasheel IH. Impact of boron carbide and graphite dual particulates addition on wear behaviour of A356 alloy metal matrix composites. Journal of Metals, Materials and Minerals, 2020; 30(4):106-112. <https://doi.org/10.55713/jmmm.v30i4.642>
- [16] Pathalinga PG, Chittappa HC, Nagaral M, Auradi V. Effect of the reinforcement particle size on the compressive strength and impact toughness of LM29 alloy B4C composites. Structural Integrity and Life, 2019;5 (7):231-236.
- [17] Sallahuddin Attar, Madeva Nagaral, Reddappa HN, V Auradi V. Effect of B4C particles addition on wear properties of Al7075 alloy composites. American Journal of Materials Science, 2015; 5(3C): 53-57.
- [18] Nagaral M, Shivananda BK, Auradi V, Kori SA. Development and mechanical wear Al2024 nano B4C composites for aerospace applications. Strength, Fracture and Complexity, 2020; 13 (1): 1-13. <https://doi.org/10.3233/SFC-190248>
- [19] Nagara M, Auradi V, Bharath V. Mechanical characterization and fractography of 100 micron sized silicon carbide particles reinforced Al6061 alloy composites. Metallurgical and Materials Engineering, 2022; 28 (1): 17-32. <https://doi.org/10.30544/639>
- [20] Chandrasekhar GL, Y Vijayakumar Y, Nagaral M, Anilkumar C. Microstructural evaluation and mechanical behavior of nano B4C reinforced Al7475 alloy metal composites. International Journal of Vehicle Structures & Systems, 2021; 13(5). <https://doi.org/10.4273/ijvss.13.5.24>
- [21] Fazil N, Venkataramana V, Nagaral M, Auradi V. Synthesis and mechanical characterization of micro B4C particulates reinforced AA2124 alloy composites. International Journal of Engineering and Technology UAE, 2018; 7 (2.23): 225-229. <https://doi.org/10.14419/ijet.v7i2.23.11954>
- [22] Nagaral M, Attar S, Reddappa HN, Auradi V, Kumar S, Raghu S. Mechanical behavior of Al7075-B4C particulate reinforced composites. Journal of Applied Mechanical Engineering, 2015; 4(6): 1000186.